

# Density functional calculations and experimental studies of the sidearm remote controlling effect in eight lariat crown ethers

Li-Hwa Lu <sup>a</sup>, Chia-Ching Su <sup>b,\*</sup>, Tian-Jye Hsieh <sup>c</sup>

<sup>a</sup> *The Center of Science Education, The Fooyin University, Ta-Liao, Kaohsiung 831, Taiwan, ROC*

<sup>b</sup> *Department of Applied Science, The ROC Naval Academy, 669, Jiun Shiaw Road, Kaohsiung 813, Taiwan, ROC*

<sup>c</sup> *Basic Medical Science Education Center, The Fooyin University, Ta-Liao, Kaohsiung 831, Taiwan, ROC*

Received 4 May 2006; received in revised form 26 July 2006; accepted 27 July 2006

Available online 14 September 2006

## Abstract

A series of eight lariat 16-crown-5 ethers (LCEs), which have the same parent macrocycle but with a different sidearm, have been synthesized. An experimental study and a quantum mechanical research, which uses the density functional theory (DFT) to calculate at the B3LYP/6-31G\* level in the Gaussian 98 and Gaussian 03 package program, were conducted on these eight LCEs. The space coordinate positions of compounds **1–4**, obtained from X-ray structural analysis, were used as initial coordinates for these theoretical calculations. The observed X-ray crystal structures of these LCEs **1–4** were compared with the optimized geometries obtained from DFT calculations. As a result, an excellent agreement between the X-ray crystallography and the four calculated compounds of conformational analysis has been found. However, the LCEs **5–8** were based on the LCEs **1–4** molecular model, which is the starting molecular structure that processes the geometric optimization calculations. Molecular mechanics and density functions were used in the theoretical study as well to determine the relative geometric stabilities of the eight compounds. The optimal geometric structures of these compounds were confirmed as well. The ionization potentials, highest occupied molecular orbital energy, lowest unoccupied molecular orbital energy, energy gaps, heat of formation, atomization energies, and vibrational frequencies of these compounds were also calculated. The results of the DFT calculations show that eight different LCEs are stable molecules with various thermodynamic properties. Thus, sidearm effect appears to cause strong influence on the metal ion binding capability.

© 2006 Elsevier B.V. All rights reserved.

**Keywords:** Lariat crown ether; DFT; B3LYP; 6-31G\*; HOMO and LUMO energies; Energy gaps

## 1. Introduction

The first macrocyclic polyether was synthesized by Lüttringhaus in 1937. He obtained dibenzo-20-crown-6 ether in low yield after the reaction of 3-(2-bromoethoxymethoxymethyl)phenol with potassium carbonate in 1-pentanol [1]. However, it was not until 1967 that Pedersen's decisive work [2] about crown ethers and cryptands became the focus of research for their remarkable selectivity in the complexation of metal ions in the past several decades. High selectivity of molecular recognition can be achieved

by designing suitable host molecules based on host–guest interaction [3]. In addition to its compatibility of shape and size, effective molecular recognition requires a precise alignment of binding groups on the receptor with complementary regions on the substrate [4]. Additionally, the molecular structure switch of crown ether has engendered great attention historically because of its ability to bind cations. They have been proposed as separation agents for removing metal ions from mixed nuclear and chemical waste [5]. In addition, these compounds are also being studied for their applications in the analytical, pharmaceutical field, and nanoscience. Therefore, one of the areas of interest is the design of drug delivery vehicles [6].

Studies, using a family of crown ethers containing oxygen, nitrogen, and sulfur atoms that identify molecular

\* Corresponding author. Tel.: +886 7 583 4700x1213/+886 7 349 4826; fax: +886 7 347 2802.

E-mail address: [ccsu@cna.edu.tw](mailto:ccsu@cna.edu.tw) (C.-C. Su).

conformations have been extensively performed with both experimental and theoretical approaches [7–12]. In addition, lariat crown ethers (LCEs) are composed of two parts, the core part and the sidearm attached to it. Because of the sidearm, crown ethers are called lariat crown ethers. They are characterized by their parent macrocyclic ring and ligating arms. Additionally, the relative ability with which crown ethers can be functionalized with pendant arm (s) containing additional donor atom (s) allows one to improve the cation binding ability and selectivity of the parent crown ether [13]. However, depending on the ring size, lariat 16-crown-5 ethers can bring about enhanced complexation, and this is due to the presence of five oxygen atoms which provide additional binding sites. In addition, the attachment of one sidearm, with potential metal ion coordination sites, to a crown ether framework produces complexing agents known as lariat crown ethers. In other words, the sidearm of the lariat crown ethers can lead to significant changes in the complexation behavior of the host molecules.

Awareness of the conformational preference of lariat crown ether is important for predicting its three-dimensional properties of molecular structures and binding affinities with guest molecules. This is especially important in the field of supramolecular chemistry and molecular recognition [14]. Unfortunately, because of their large size and complexity, there are few calculations on LCEs in the literature. In recent years, scientific studies using the DFT calculations have become more significant. In fact, theoretical and experimental studies are

closely correlated [15]. Without theoretical research, experimental results alone cannot produce methods to allow systematic analyses. Likewise, without experimental studies, the accuracy of theoretical studies cannot be proven. These two approaches therefore supplement each other. In addition, theoretical calculations have gradually become the mainstream of scientific research in the recent decade.

We hereby report the density functional theory geometry optimization at the B3LYP/6-31G\* level of theory for the eight different LCEs. Our main aim is to examine the effects of the side arm on molecular conformation. Recent reports of the theoretical calculations of molecules [16–26] have shown that the B3LYP method, in the Gaussian 98 or Gaussian 03 package program together with the 6-31G\* basis set function (BSF) of the DFT, can be a useful tool in providing adequately accurate conformational analysis [27–30]. Furthermore, and importantly, this study showcases a comparison of theoretical method that should prove useful to those interested in modeling eight LCEs. This research included those using the B3LYP/6-31G\* method as well to conduct calculations for the determination of relative geometric structures, molecular orbital energy, and other thermodynamic properties of eight LCEs. Theoretical calculations were also used to understand the experimental findings. The eight LCEs were selected to check on the accuracy of theoretical analysis versus experimental results. This systematic research about conformational analysis is also helpful to understand the influences of the different sidearms of LCEs on the metal ions selectivity.

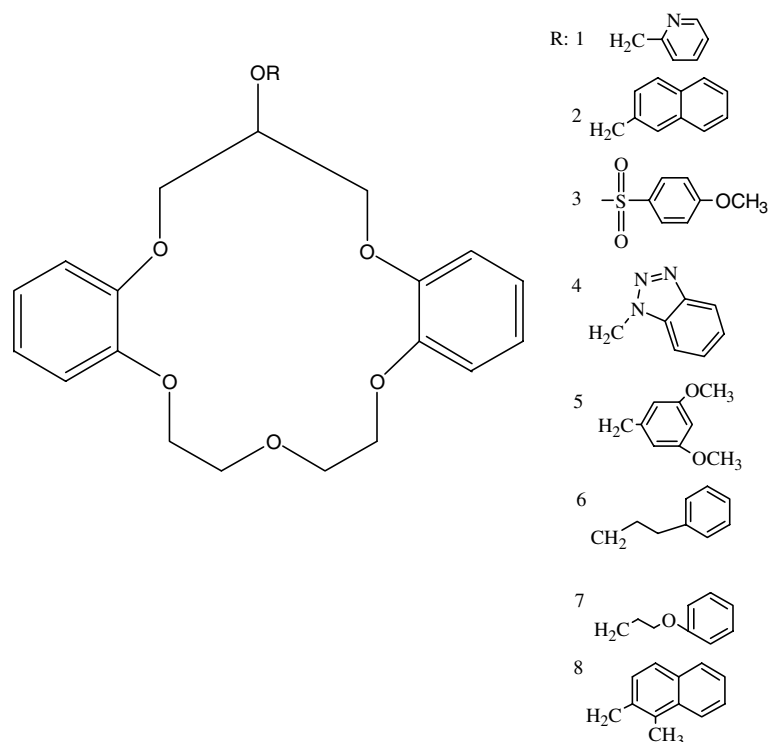


Fig. 1. Structure of eight lariat crown ethers.

## 2. Experimental details

### 2.1. Reagents and chemicals

All chemicals used for the synthesis were of available purity and were used without any further purification. Only analytical reagent grade chemicals were used in the preparation of the different eight LCEs. Hydroxy-*sym*-dibenzo-16-crown-5-ether was synthesized according to literature procedures [31] and used after recrystallization from chloroform–hexane (1:5, V:V).

### 2.2. Synthesis of 2'-picoyl *sym*-dibenzo-16-crown-5-ether **1**

Hydroxy-*sym*-dibenzo-16-crown-5-ether (1.73 g, 5 mmol) was dissolved in 50 mL anhydrous THF. NaH (0.8 g, 20 mmol) was added under nitrogen and the reaction mixture was heated under reflux for 30–40 min. After the addition of 2-picoyl chloride hydrochloride (5 mmol), the mixture was then heated (under reflux) for another 6 h. Deionized water was then added slowly to destroy the excess NaH and quench the reaction. The reaction mixture was then purified by column chromatography (silica gel, 70–230 mesh, CHCl<sub>3</sub> eluent) to give the desired product **1** in

85% (1.86 g) yield, mp 122.0–123.0 °C. MS (EI, 70 eV): *m/z* 437.2 (M<sup>+</sup>, 17%), 328.2 (48%), 148.1 (78%), 135.9 (100%), 121.0 (76%), 91.9 (88%). Elemental analysis: Calcd (found) for C<sub>25</sub>H<sub>27</sub>NO<sub>6</sub>: C, 68.62 (68.68); H, 6.22 (6.33); N, 3.20 (3.19). <sup>1</sup>H NMR (CDCl<sub>3</sub>): δ 3.92 (m, 4H, OCH<sub>2</sub>CH<sub>2</sub>OCH<sub>2</sub>CH<sub>2</sub>O), 4.15 (m, 4H, OCH<sub>2</sub>CH<sub>2</sub>OCH<sub>2</sub>CH<sub>2</sub>O), 4.29 (m, 3H, OCHH'CHCHH'O), 4.40 (dd, <sup>2</sup>J=8.8 Hz, <sup>3</sup>J=3.4 Hz, 2H, OCHH'CHCHH'O), 5.01 (s, 2H, CH<sub>2</sub>Py), 6.86 (m, 4H, benzo group), 6.97 (m, 4H, benzo group), 7.19 (m, 1H, 5 position H of Py), 7.67 (m, 2H, 3 and 4 position H of Py), 8.55 (d, <sup>3</sup>J=4.4 Hz, 1H, 6 position H of Py).

### 2.3. Synthesis of methylnaphthalene *sym*-dibenzo-16-crown-5-ether **2**

Hydroxy-*sym*-dibenzo-16-crown-5-ether (1.73 g, 5 mmol) was dissolved in 50 mL anhydrous THF. NaH (0.8 g, 20 mmol) was added under nitrogen and the reaction mixture was heated under reflux for 30–40 min. After the addition of the 1-(chloromethyl) naphthalene (5 mmol), the mixture was heated (under reflux) for 3 h. The excess NaH was then destroyed with water, and the reaction mixture was purified as describe in **1** to give **2** a 80% (1.94 g) yield, mp 91.0–92.0 °C. MS (EI, 70 eV): *m/z* 486.3

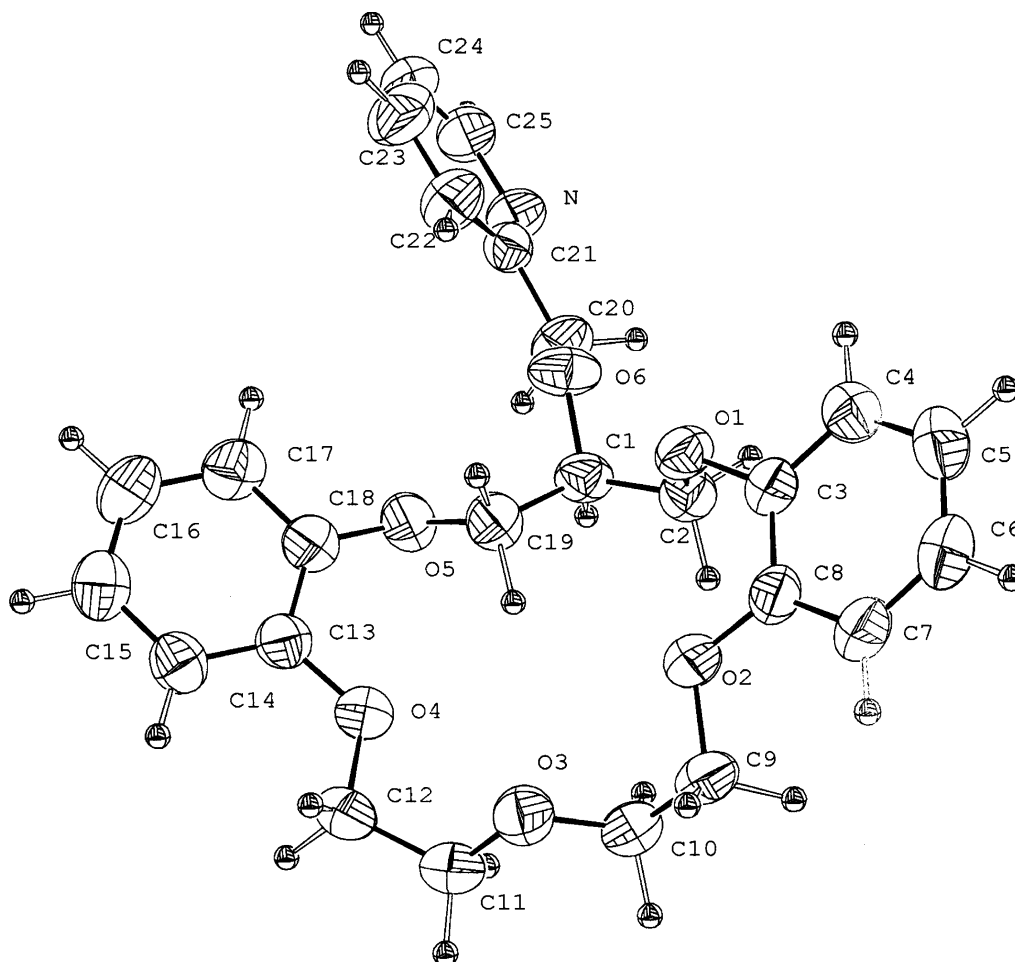


Fig. 2. ORTEP diagram of lariat crown ether **1**.

( $M^+$ , 55%), 330.2 (4%), 194.3 (6%), 141.1 (100%), 121.1 (23%), 115.1 (13%), 109.1 (5%). Elemental analysis: Calcd (found) for  $C_{30}H_{30}O_6$ ; C, 74.06 (74.20); H, 6.21 (6.23).  $^1H$  NMR ( $CDCl_3$ ):  $\delta$  3.93 (m, 4H,  $OCH_2CH_2OCH_2CH_2O$ ), 4.16 (m, 2H,  $OCHH'CHCHH'O$ ), 1H,

$OCHH'CHCHH'O$ , 4H,  $OCH_2CH_2OCH_2CH_2O$ , 4.32 (m, 2H,  $OCHH'CHCHH'O$ ), 5.06 (s, 2H,  $CH_2$ ), 6.84–7.00 (m, 8H, benzo group), 7.49 (m, 2H, naphthalene group), 7.61 (dd, 1H, naphthalene group), 7.86 (m, 4H, naphthalene group).

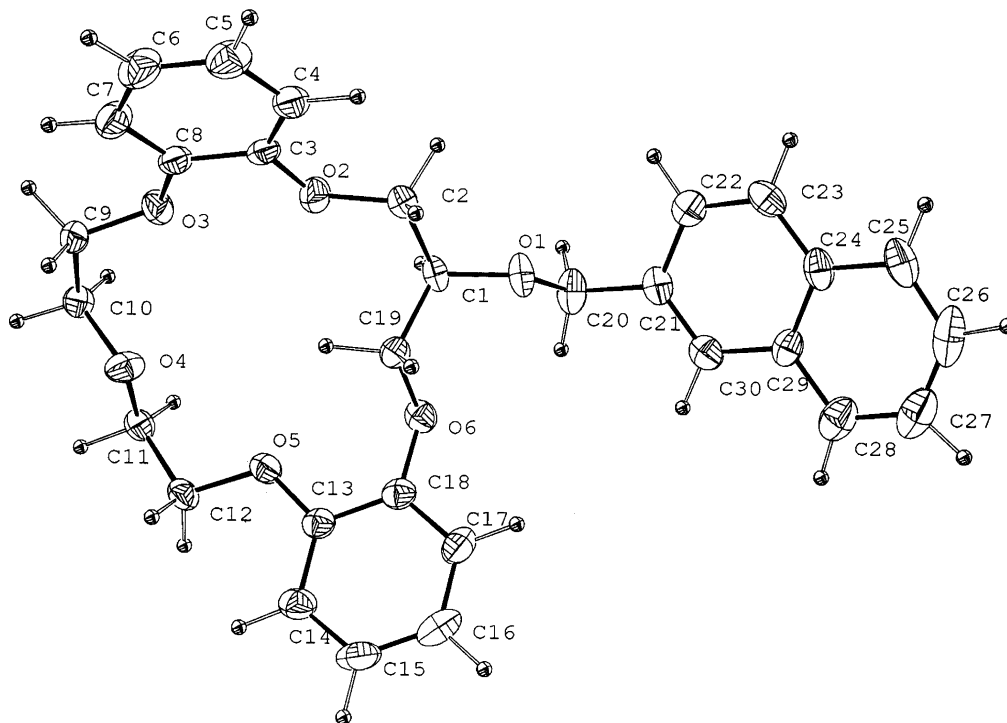


Fig. 3. ORTEP diagram of lariat crown ether 2.

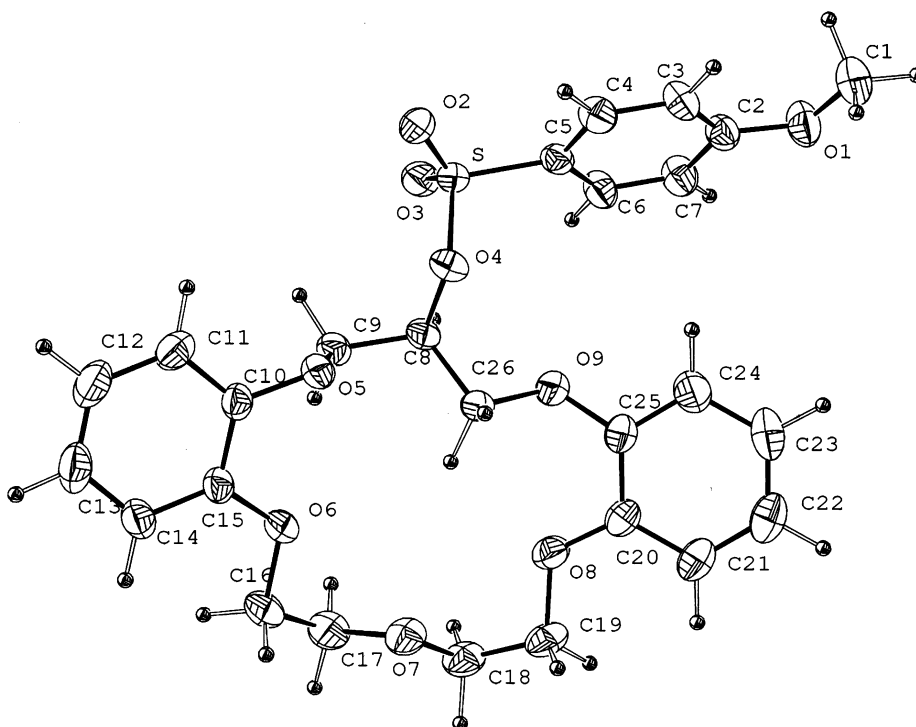
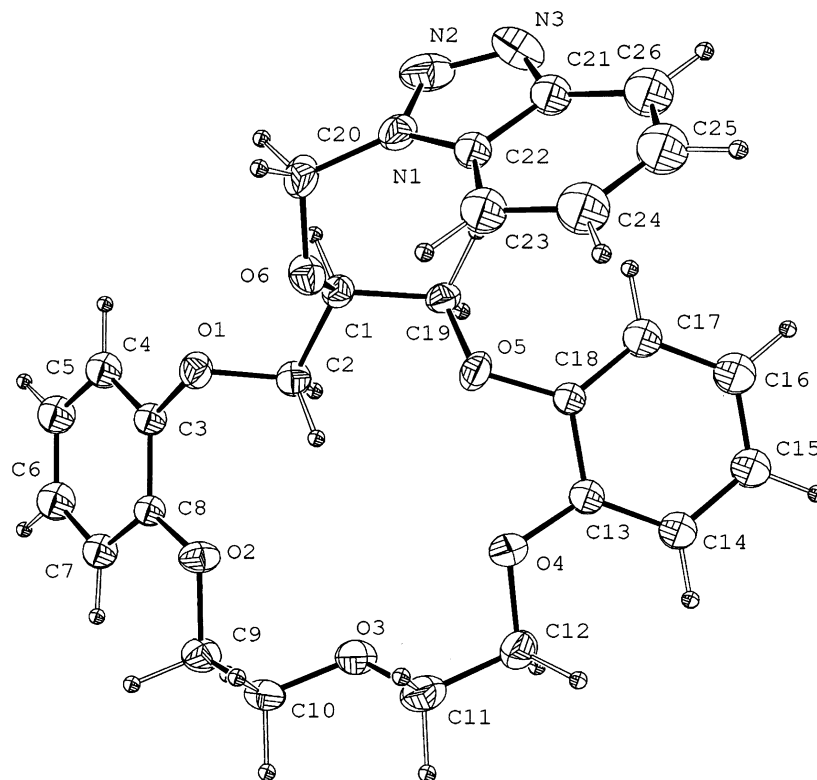


Fig. 4. ORTEP diagram of lariat crown ether 3.

Fig. 5. ORTEP diagram of lariat crown ether **4**.

#### 2.4. Synthesis of 4-methoxybenzenesulfonyl sym-dibenzo-16-crown-5-ether **3**

Hydroxy-sym-dibenzo-16-crown-5-ether (1.73 g, 5 mmol) was dissolved in 50 mL anhydrous THF. NaH (0.8 g, 20 mmol) was added under nitrogen and the reaction mixture was heated under reflux for 30–40 min. Then, 4-methoxybenzenesulfonyl chloride (5 mmol) was added to this solution. Heating of the mixture was then continued under the reflux for 1 h. Next, the excess NaH was destroyed with water, and the reaction mixture was purified as describe in **1** to give **3** a 80% (2.06 g) yield, mp 112.0–113.0 °C. MS (EI, 70 eV):  $m/z$  516.3 ( $M^+$ , 100%), 171.1 (35%), 136.1 (43%), 121.1 (56%), 107.1 (23%), 77.1 (15%). Elemental analysis: Calcd (found) for  $C_{26}H_{28}SO_9$ ; C, 60.45 (60.50); H, 5.46 (5.45).  $^1H$  NMR ( $CDCl_3$ ):  $\delta$  3.85 (s, 3H,  $OCH_3$ ), 3.88 (t, 4H,  $^3J=6.84$  Hz,  $OCH_2CH_2OCH_2CH_2O$ ), 4.10 (t, 4H,  $OCH_2CH_2OCH_2CH_2O$ ), 4.35 (qq, 4H,  $OCHH'CHCHH'O$ ), 5.08 (q, 1H,  $OCHH'CHCHH'O$ ), 6.84–7.00 (m, 10H, benzo group), 7.94 (dd, 2H, benzo group).

#### 2.5. Synthesis of 1-(methyl)-1H-benzotriazole sym-dibenzo-16-crown-5-ether **4**

Hydroxy-sym-dibenzo-16-crown-5-ether (1.73 g, 5 mmol) was dissolved in 50 mL anhydrous THF. *t*-BuOK (1.12 g, 10 mmol) was added under nitrogen and the reaction mixture was kept at room temperature for 5 h. After the addition of the 1-(chloromethyl)-1H-benzotriazole (5 mmol), the mixture was kept at room temperature for 5 h. Then, the

excess *t*-BuOK was destroyed with water, and the reaction mixture was purified as describe in **1** to give **4** a 70% (1.67 g) yield, mp 98.0–99.0 °C. MS (EI, 70 eV):  $m/z$  477.3 ( $M^+$ , 100%), 328.1 (9%), 149.1 (11%), 136.1 (29%), 132.0 (55%), 121.1 (48%), 77.1 (29%). Elemental analysis: Calcd (found) for  $C_{26}H_{27}N_3O_6$ ; C, 65.40 (65.34); H, 5.70 (5.69).  $^1H$  NMR ( $CDCl_3$ ):  $\delta$  3.93 (m, 4H,  $OCH_2CH_2OCH_2CH_2O$ ), 4.16 (m, 3H,  $OCHH'CHCHH'O$ , 4H,  $OCH_2CH_2OCH_2CH_2O$ ), 4.32 (m, 2H,  $OCHH'CHCHH'O$ ), 6.38 (s, 2H,  $CH_2$ ), 6.84–7.00 (m, 8H, benzo group), 7.41 (t, 1H, aromatic group), 7.50 (t, 1H, aromatic group), 7.80 (d, 1H, aromatic group), 8.07 (d, 1H, aromatic group).

#### 2.6. Synthesis of 3,5-dimethoxybenzyl sym-dibenzo-16-crown-5-ether **5**

Hydroxy-sym-dibenzo-16-crown-5-ether (1.73 g, 5 mmol) was dissolved in 50 mL anhydrous THF. NaH (0.8 g, 20 mmol) was added under nitrogen and the reaction mixture was heated under reflux for 30–40 min. After which, 3,5-dimethoxybenzyl chloride (5 mmol) was added and the reaction mixture was heated under reflux for 1 h. The excess NaH was then destroyed with water, and the reaction mixture was purified as describe in **1** to give **5** a 80% (1.98 g) yield, mp 99.0–100.0 °C. MS (EI, 70 eV):  $m/z$  496.1 ( $M^+$ , 42%), 206.9 (7%), 151.0 (100%), 121.0 (25%), 77.1 (10%). Elemental analysis: Calcd (found) for  $C_{28}H_{32}O_8$ ; C, 67.73 (67.67); H, 6.50 (6.46).  $^1H$  NMR ( $CDCl_3$ ):  $\delta$  3.79 (s, 6H,  $OCH_3$ ), 3.93 (m, 4H,  $OCH_2CH_2OCH_2CH_2O$ ), 4.16 (m, 2H,  $OCHH'CHCHH'O$ , 1H,  $OCHH'CHCHH'O$ , 4H,  $OCH_2$

CH<sub>2</sub>OCH<sub>2</sub>C H<sub>2</sub>O), 4.32 (m, 2H, OCHH'CHCHH'O), 4.84 (s, 2H, CH<sub>2</sub>), 6.40 (t, 1H, benzo group), 6.63 (d, 2H, benzo group), 6.84–7.00 (m, 8H, benzo group).

### 2.7. Synthesis of 3-phenylpropyl sym-dibenzo-16-crown-5-ether **6**

Hydroxy-sym-dibenzo-16-crown-5-ether (1.73 g, 5 mmol) was dissolved in 50 mL anhydrous THF. NaH (0.8 g, 20 mmol) was added under nitrogen and the reaction mixture was heated under reflux for 30–40 min. Then, 3-phenylpropyl bromide (5 mmol) was added to this solution. Heating was then continued under the reflux for 1 h. Then, the excess NaH was destroyed with water, and the reaction mixture was purified as describe in **1** to give **6** a 79% (1.83 g) yield, mp 84.0–85.0 °C. MS (EI, 70 eV): *m/z* 464.2 (M<sup>+</sup>, 13%), 169.1 (10%), 155.0 (100%), 121.0 (8%), 77.0 (3%). Elemental analysis: Calcd (found) for C<sub>28</sub>H<sub>32</sub>O<sub>6</sub>: C, 72.39 (72.28); H, 6.94 (6.81). <sup>1</sup>H NMR (CDCl<sub>3</sub>): δ 1.55 (q, 2H, OCH<sub>2</sub>CH<sub>2</sub>CH<sub>2</sub>Ph), 2.79 (t, 2H, OCH<sub>2</sub>CH<sub>2</sub>CH<sub>2</sub>Ph), 3.79 (t, 2H, OCH<sub>2</sub>CH<sub>2</sub>CH<sub>2</sub>Ph), 3.93 (m, 4H, OCH<sub>2</sub>CH<sub>2</sub>OCH<sub>2</sub>C H<sub>2</sub>O), 4.16 (m, 2H, OCHH'CHCHH'), 1H, OCHH'

Table 1  
Crystallographic data and optimized structure of lariat crown ether **1** located using B3LYP/6-31G\* calculations for atomic bond lengths (Å)

Atomic bond lengths (Å)	Crystallographic data	B3LYP/6-31G*
O1–C1	1.433(4)	1.432
O1–C3	1.389(4)	1.374
O2–C8	1.359(5)	1.369
O2–C9	1.440(4)	1.421
O3–C10	1.395(5)	1.411
O3–C11	1.427(5)	1.415
O4–C12	1.439(5)	1.419
O4–C13	1.362(4)	1.368
O5–C18	1.372(4)	1.372
O5–C19	1.459(4)	1.438
O6–C1	1.433(4)	1.424
O6–C20	1.393(7)	1.412
N1–C21	1.333(5)	1.342
N–C25	1.355(5)	1.337
C1–C2	1.509(5)	1.528
C1–C19	1.486(5)	1.522
C3–C4	1.373(5)	1.392
C3–C8	1.392(5)	1.414
C4–C5	1.386(5)	1.398
C5–C6	1.376(7)	1.391
C6–C7	1.381(6)	1.399
C7–C8	1.400(5)	1.398
C9–C10	1.500(6)	1.516
C11–C12	1.493(6)	1.516
C13–C14	1.381(5)	1.397
C13–C18	1.396(5)	1.413
C14–C15	1.383(6)	1.399
C15–C16	1.366(7)	1.392
C16–C17	1.386(6)	1.398
C17–C18	1.378(5)	1.392
C20–C21	1.505(5)	1.513
C21–C22	1.366(5)	1.398
C22–C23	1.383(6)	1.394
C23–C24	1.349(7)	1.394
C24–C25	1.354(7)	1.396

CHCHH', 4H, OCH<sub>2</sub>CH<sub>2</sub>OCH<sub>2</sub>CH<sub>2</sub>O), 4.32 (m, 2H, OCHH'CHCHH'), 6.83–7.00 (m, 8H, benzo group), 7.18–7.32 (m, 5H, benzo group).

### 2.8. Synthesis of 3-phenoxypropyl sym-dibenzo-16-crown-5-ether **7**

Hydroxy-sym-dibenzo-16-crown-5-ether (1.73 g, 5 mmol) was dissolved in 50 mL anhydrous THF. *t*-BuOK (1.12 g, 10 mmol) was added under nitrogen and the reaction mixture was kept at room temperature for 5 h. Afterward, 3-phenoxypropyl bromide (20 mmol) was added to this solution, in which the reaction continued to be placed under room temperature for another 3 h. The excess *t*-BuOK was then destroyed with water, and the reaction mixture was purified as describe in **1** to give **7** a 50% (1.2 g) yield, mp 85.0–86.0 °C. MS (EI, 70 eV): *m/z* 480.4 (M<sup>+</sup>, 100%), 149.2 (4%), 136.1 (5%), 121.1 (33%), 107.1 (21%),

Table 2  
Crystallographic data and optimized structure of lariat crown ether **2** located using B3LYP/6-31G\* calculations for atomic bond lengths (Å)

Atomic bond lengths (Å)	Crystallographic data	B3LYP/6-31G*
O1–C1	1.411(6)	1.424
O1–C20	1.408(6)	1.430
O2–C2	1.427(6)	1.424
O2–C3	1.367(6)	1.369
O3–C8	1.372(6)	1.367
O3–C9	1.414(6)	1.423
O4–C10	1.413(5)	1.415
O4–C11	1.412(6)	1.423
O5–C12	1.432(6)	1.425
O5–C13	1.363(6)	1.364
O6–C18	1.382(6)	1.379
O6–C19	1.440(6)	1.436
C1–C2	1.510(7)	1.532
C1–C19	1.504(7)	1.524
C3–C4	1.386(7)	1.394
C3–C8	1.397(7)	1.419
C4–C5	1.388(8)	1.401
C5–C6	1.352(9)	1.388
C6–C7	1.398(8)	1.401
C7–C8	1.362(8)	1.393
C9–C10	1.502(7)	1.524
C11–C12	1.485(7)	1.522
C13–C14	1.382(7)	1.396
C13–C18	1.401(8)	1.412
C14–C15	1.389(8)	1.399
C15–C16	1.367(10)	1.393
C16–C17	1.381(9)	1.399
C17–C18	1.374(7)	1.391
C20–C21	1.497(7)	1.508
C21–C22	1.405(8)	1.423
C21–C30	1.360(7)	1.378
C22–C23	1.364(8)	1.374
C23–C24	1.407(8)	1.422
C24–C25	1.434(7)	1.420
C24–C29	1.416(8)	1.432
C25–C26	1.377(10)	1.377
C26–C27	1.391(12)	1.416
C27–C28	1.355(10)	1.377
C28–C29	1.407(8)	1.421
C29–C30	1.421(8)	1.421

77.1 (12%). Elemental analysis: Calcd (found) for  $C_{28}H_{32}O_7$ ; C, 69.98 (69.90); H, 6.71 (6.72).  $^1H$  NMR ( $CDCl_3$ ):  $\delta$  2.14 (q, 2H,  $OCH_2CH_2CH_2O$ ), 3.97 (t, 2H,  $OCH_2CH_2CH_2$ , m, 4H,  $OCH_2CH_2OCH_2CH_2O$ ), 4.16 (m, 3H,  $OCHH'CHCHH'$ , 4H,  $OCH_2CH_2OCH_2CH_2O$ ), 2H, t,  $OCH_2CH_2CH_2O$ ), 4.32 (m, 2H,  $OCHH'CHCHH'$ ), 6.84–7.00 (m, 11H, benzo group), 7.28 (m, 2H, benzo group).

### 2.9. Synthesis of methyl-2-methylnaphthalene sym-dibenzo-16-crown-5-ether **8**

Hydroxy-sym-dibenzo-16-crown-5-ether (1.73 g, 5 mmol) was dissolved in 50 mL anhydrous THF. NaH (0.8 g, 20 mmol) was added under nitrogen and the reaction mixture was heated under reflux for 30–40 min. After the addition of the 1-chloromethyl-2-methylnaphthalene (5 mmol), the mixture was heated (under reflux) for 3 h. Then, the excess NaH was destroyed with water, and the

reaction mixture was purified as describe in **1** to give **8** a 80% (2.00 g) yield, mp 144.0–145.0 °C. MS (EI, 70 eV):  $m/z$  500.2 ( $M^+$ , 13%), 169.1 (10%), 155.0 (100%), 121.0 (8%), 77 (3%). Elemental analysis: Calcd (found) for  $C_{31}H_{32}O_6$ ; C, 74.06 (74.20); H, 6.21 (6.23).  $^1H$  NMR ( $CDCl_3$ ):  $\delta$  2.67 (s, 3H,  $CH_3$ ), 3.93 (m, 4H,  $OCH_2CH_2OCH_2CH_2O$ ), 4.16 (m, 2H,  $OCHH'CHCHH'O$ , 1H,  $OCHH'CHCHH'O$ , 4H,  $OCH_2CH_2OCH_2CH_2O$ ), 4.32 (m, 2H,  $OCHH'CHCHH'O$ ), 5.38 (s, 2H,  $CH_2$ ), 6.84–7.00 (m, 8H, benzo group), 7.36 (m, 3H, naphthalene group), 7.72 (m, 2H, naphthalene group), 8.38 (d, 1H, naphthalene group).

### 2.10. Production of single crystals of four LCEs

Single crystals of LCEs **1–4** were produced by initially heating the four 16-crown-5 ethers (0.50 g) in *n*-hexane (10 mL). Chloroform was then slowly added to the mixture until the compound fully dissolved. Magnesium

Table 3  
Crystallographic data and optimized structure of lariat crown ether **3** located using B3LYP/6-31G\* calculations for atomic bond lengths (Å)

Atomic bond lengths (Å)	Crystallographic data	B3LYP/6-31G*
S–O2	1.431(4)	1.461
S–O3	1.412(4)	1.466
S–O4	1.577(3)	1.643
S–C5	1.743(4)	1.778
O1–C1	1.414(7)	1.422
O1–C2	1.354(6)	1.359
O4–C8	1.463(5)	1.459
O5–C9	1.418(5)	1.431
O5–C10	1.381(5)	1.375
O6–C15	1.360(6)	1.370
O6–C16	1.437(6)	1.421
O7–C17	1.402(6)	1.412
O7–C18	1.418(6)	1.415
O8–C19	1.442(6)	1.420
O8–C20	1.360(6)	1.367
O9–C25	1.382(5)	1.376
O9–C26	1.423(5)	1.438
C2–C3	1.372(7)	1.401
C2–C7	1.395(7)	1.408
C3–C4	1.364(7)	1.396
C4–C5	1.376(7)	1.391
C5–C6	1.391(6)	1.402
C6–C7	1.356(7)	1.385
C8–C9	1.505(6)	1.521
C8–C26	1.506(6)	1.519
C10–C11	1.372(7)	1.391
C10–C15	1.398(7)	1.413
C11–C12	1.388(8)	1.398
C12–C13	1.349(10)	1.391
C13–C14	1.384(8)	1.399
C14–C15	1.390(6)	1.397
C16–C17	1.489(8)	1.516
C18–C19	1.475(8)	1.515
C20–C21	1.380(7)	1.397
C20–C25	1.400(7)	1.413
C21–C22	1.371(7)	1.399
C22–C23	1.375(10)	1.392
C23–C24	1.395(8)	1.398
C24–C25	1.375(7)	1.392

Table 4  
Crystallographic data and optimized structure of lariat crown ether **4** located using B3LYP/6-31G\* calculations for atomic bond lengths (Å)

Atomic bond lengths (Å)	Crystallographic data	B3LYP/6-31G*
O1–C2	1.420(8)	1.434
O1–C3	1.396(8)	1.380
O2–C8	1.374(8)	1.366
O2–C9	1.443(9)	1.428
O3–C10	1.417(10)	1.424
O3–C11	1.416(9)	1.415
O4–C12	1.423(9)	1.422
O4–C13	1.355(9)	1.366
O5–C18	1.376(8)	1.366
O5–C19	1.420(8)	1.422
O6–C1	1.442(9)	1.432
O6–C20	1.418(9)	1.406
N1–N2	1.347(11)	1.372
N1–C20	1.457(10)	1.455
N1–C22	1.356(6)	1.369
N2–N3	1.310(12)	1.291
N3–C21	1.375(11)	1.382
C1–C2	1.512(10)	1.527
C1–C19	1.515(10)	1.526
C3–C4	1.384(10)	1.392
C3–C8	1.370(10)	1.412
C4–C5	1.406(11)	1.398
C5–C6	1.350(12)	1.393
C6–C7	1.381(11)	1.398
C7–C8	1.390(10)	1.397
C9–C10	1.495(11)	1.523
C11–C12	1.493(12)	1.525
C13–C14	1.372(10)	1.393
C13–C18	1.407(10)	1.419
C14–C15	1.383(11)	1.402
C15–C16	1.359(12)	1.388
C16–C17	1.398(11)	1.402
C17–C18	1.366(10)	1.393
C21–C22	1.380(11)	1.409
C21–C26	1.414(12)	1.404
C22–C23	1.393(11)	1.403
C23–C24	1.383(13)	1.387
C24–C25	1.371(14)	1.417
C25–C26	1.323(14)	1.386

sulfate was then added and the mixture was filtered while still hot. The filtered product was then put into a crystal-growing bottle and *n*-hexane vapor was diffused into the product until a perfect crystal was produced. The structure of the resulting single crystals was then analyzed by X-ray crystallography. Data were collected using a Nonius CAD-4 diffractometer with graphite-monochromated Mo-K $\alpha$  radiation at 25 °C. Atomic scattering factors were taken from the International Tables for X-ray crystallography, and data reduction and structural refinement were performed using the NRCVAX packages. Cell parameters for **1–4** were obtained from 25 reflections with  $2\theta$  at 21.08–24.94°, 19.58–24.70°, 21.96–28.28°, and 11.98–22.92°, respectively.

Table 5  
Crystallographic data and optimized structure of lariat crown ether **1** located using B3LYP/6-31G\* calculations of atomic torsion angle (°)

Atomic torsion angle (°)	Crystallographic data	B3LYP/6-31G*
C2–O1–C3	113.4(3)	117.0
C8–O2–C9	117.7(3)	118.5
C10–O3–C11	112.1(3)	113.2
C12–O4–C13	117.8(3)	119.1
C18–O5–C19	115.8(3)	116.3
C1–O6–C20	115.1(3)	114.8
C21–N–C25	116.6(3)	117.7
O6–C1–C2	110.8(3)	112.2
O6–C–C19	108.2(3)	107.8
C2–C1–C19	112.5(3)	111.3
O1–C2–C1	108.8(3)	108.2
O1–C3–C4	119.3(3)	118.8
O1–C3–C8	119.7(3)	121.3
C4–C3–C8	120.9(3)	119.7
C3–C4–C5	119.9(4)	120.8
C4–C5–C6	119.8(4)	119.4
C5–C6–C7	121.0(3)	120.4
C6–C7–C8	119.5(4)	120.3
O2–C8–C3	116.9(3)	116.1
O2–C8–C7	124.2(3)	124.7
C3–C8–C7	119.0(4)	119.3
O2–C9–C10	108.0(3)	108.6
O3–C10–C9	109.1(3)	109.6
O3–C11–C12	108.3(5)	108.9
O4–C12–C11	106.2(3)	107.4
O4–C13–C14	124.4(3)	124.7
O4–C13–C18	115.6(3)	115.7
C14–C13–C18	120.0(3)	119.6
C13–C14–C15	120.0(4)	120.1
C14–C15–C16	120.3(4)	120.4
C15–C16–C17	120.1(4)	119.6
C16–C17–C18	120.5(4)	120.8
O5–C18–C13	122.1(3)	121.5
O5–C18–C17	118.6(3)	118.9
C13–C18–C17	119.1(3)	119.5
O5–C19–C1	106.3(3)	107.2
O6–C20–C21	109.9(3)	110.1
N–C21–C20	113.4(3)	114.7
N–C21–C22	123.2(3)	123.1
C20–C21–C22	123.3(3)	122.2
C21–C22–C23	118.3(4)	118.4
C22–C23–C24	119.4(4)	119.1
C23–C24–C25	119.3(4)	118.0
N–C25–C24	123.1(4)	123.7

### 3. Computational method

#### 3.1. Calculation methods and input

All theoretical calculations were performed with the Gaussian98 and Gaussian03 program packages. The density function calculations (DFT) used the B3LYP method

Table 6  
Crystallographic data and optimized structure of lariat crown ether **2** located using B3LYP/6-31G\* calculations of atomic torsion angle (°)

Atomic torsion angle (°)	Crystallographic data	B3LYP/6-31G*
C1–O1–C20	117.1(4)	115.3
C2–O2–C3	118.6(4)	117.9
C8–O3–C9	117.2(4)	119.0
C10–O4–C11	112.5(3)	113.7
C12–O5–C13	118.0(4)	119.7
C18–O6–C19	112.8(3)	115.0
O1–C1–C2	104.0(4)	104.7
O1–C1–C19	110.7(4)	112.1
C2–C1–C19	109.5(4)	111.1
O2–C2–C1	108.3(4)	109.0
O2–C3–C4	125.4(5)	124.7
O2–C3–C8	115.7(4)	116.0
C4–C3–C8	118.8(5)	119.3
C3–C4–C5	120.2(5)	120.6
C4–C5–C6	120.2(5)	120.1
C5–C6–C7	120.4(5)	119.9
C6–C7–C8	119.7(5)	120.5
O3–C8–C3	114.5(5)	115.7
O3–C8–C7	124.9(5)	124.7
C3–C8–C7	120.6(5)	119.6
O3–C9–C10	107.4(4)	108.9
O4–C10–C9	106.7(4)	114.0
O4–C11–C12	108.1(4)	108.0
O5–C12–C11	107.6(4)	104.7
O5–C13–C14	124.6(5)	124.9
O5–C13–C18	115.6(4)	115.5
C14–C13–C18	119.9(5)	119.6
C13–C14–C15	119.1(5)	119.9
C14–C15–C16	121.1(5)	120.5
C15–C16–C17	119.8(5)	119.6
C16–C17–C18	120.4(5)	120.4
O6–C18–C13	120.9(4)	120.1
O6–C18–C17	119.4(5)	120.0
C13–C18–C17	119.7(5)	119.9
O6–C19–C1	109.8(4)	109.3
O1–C20–C21	105.3(4)	108.7
C20–C21–C22	118.8(5)	119.6
C20–C21–C30	122.2(5)	121.2
C22–C21–C30	118.9(5)	119.1
C21–C22–C23	121.5(5)	120.8
C22–C23–C24	120.6(5)	121.1
C23–C24–C25	122.0(5)	122.5
C23–C24–C29	118.5(5)	118.5
C25–C24–C29	119.5(5)	118.9
C24–C25–C26	118.6(6)	120.8
C25–C26–C27	120.8(6)	120.2
C26–C27–C28	121.7(6)	120.3
C27–C28–C29	120.1(6)	120.9
C24–C29–C28	119.2(5)	118.8
C24–C29–C30	119.0(5)	118.9
C28–C29–C30	121.7(5)	122.3
C21–C30–C29	121.3(3)	121.6

together with a 6-31G\* basis set function in Gaussian. The initial three-dimensional coordinates of the compounds **1–4** that were used in the calculation were obtained from the X-ray structural analysis. However, for LCEs **5–8**, the starting molecular structures were based on LCEs **1–4**.

### 3.2. Geometry optimization

The results of the DFT calculations were used to confirm the quality of the input coordinate data. If unreasonable data were used, either the geometric symmetry of the molecules would be destroyed or unusual bond length or bond angle would be produced. Any of these errors would

Table 7  
Crystallographic data and optimized structure of lariat crown ether **3** located using B3LYP/6-31G\* calculations of atomic torsion angle (°)

Atomic torsion angle (°)	Crystallographic data	B3LYP/6-31G*
O2–S–C3	119.7(2)	120.1
O2–S–O4	104.4(2)	118.0
O2–S–C5	109.0(2)	108.9
O3–S–O4	109.6(2)	108.3
O3–S–C5	109.9(2)	109.9
O4–S–C5	103.0(2)	99.8
C1–O1–C2	118.3(4)	118.6
S–O4–C8	121.9(3)	119.2
C9–O5–C10	114.8(3)	117.0
C15–O6–C16	117.1(3)	118.6
C17–O7–C18	110.7(4)	113.3
C19–O8–C20	118.4(4)	119.0
C25–O9–C26	119.3(3)	115.9
O1–C2–C3	124.6(5)	124.6
O1–C2–C7	115.8(4)	115.4
C3–C2–C7	119.6(6)	120.1
C2–C3–C4	119.8(4)	119.6
C3–C4–C5	120.9(4)	119.8
S–C5–C4	119.7(3)	119.4
S–C5–C6	120.7(4)	119.6
C4–C5–C6	119.5(4)	121.0
C5–C6–C7	119.6(4)	119.2
C2–C7–C6	120.5(4)	120.3
O4–C8–C9	109.0(3)	110.8
O4–C8–C26	107.4(3)	106.8
C9–C8–C26	114.2(4)	112.5
O5–C9–C8	108.5(3)	108.5
O5–C10–C11	120.4(4)	118.8
O5–C10–C15	119.5(4)	121.2
C11–C10–C15	120.0(4)	119.8
C10–C11–C12	120.1(5)	120.7
C11–C12–C13	120.1(5)	119.5
C12–C13–C14	121.0(5)	120.5
C13–C14–C15	119.6(5)	120.2
O6–C15–C10	115.2(4)	116.0
O6–C15–C14	125.7(4)	124.7
C10–C15–C14	119.0(4)	119.3
O6–C16–C17	107.3(4)	108.5
O7–C17–C16	110.1(4)	109.6
O7–C18–C19	109.8(4)	108.7
O8–C19–C18	106.8(4)	107.4
O8–C20–C21	124.6(5)	124.7
O8–C20–C25	115.9(4)	115.8
C21–C20–C25	119.5(5)	119.5
C20–C21–C22	119.9(5)	120.1
C21–C22–C23	121.3(5)	120.4
C22–C23–C24	119.2(5)	119.6
C23–C24–C25	120.0(5)	120.7
O9–C25–C20	122.6(4)	121.1
O9–C25–C24	117.0(5)	119.2
C20–C25–C24	120.1(4)	119.7
O9–C26–C8	105.4(3)	107.5

Table 8  
Crystallographic data and optimized structure of lariat crown ether **4** located using B3LYP/6-31G\* calculations of atomic torsion angle (°)

Atomic torsion angle (°)	Crystallographic data	B3LYP/6-31G*
C2–O1–C3	115.7(5)	115.2
C8–O2–C9	117.7(5)	119.1
C10–O3–C11	111.2(6)	114.0
C12–O4–C13	117.2(6)	119.4
C18–O5–C19	117.0(5)	118.9
C1–O6–C20	115.6(6)	115.4
N2–N1–C20	119.3(7)	120.4
N2–N1–C22	111.0(6)	109.8
C20–N1–C22	129.3(7)	129.6
N1–N2–N3	108.5(6)	109.4
N2–N3–C21	107.5(7)	108.5
O6–C1–C2	108.3(6)	110.8
O6–C1–C19	111.8(5)	107.8
C2–C1–C19	110.5(6)	111.2
O1–C2–C1	109.5(5)	108.7
O1–C3–C4	116.6(6)	119.0
O1–C3–C8	122.0(6)	121.1
C4–C3–C8	121.4(6)	119.8
C3–C4–C5	118.5(7)	120.5
C4–C5–C6	119.9(7)	119.6
C5–C6–C7	121.3(7)	120.4
C6–C7–C8	119.6(7)	120.2
O2–C8–C3	117.0(6)	116.3
O2–C8–C7	123.7(6)	124.3
C3–C8–C7	119.2(6)	119.4
O2–C9–C10	108.1(6)	105.5
O3–C10–C9	109.6(6)	107.4
O3–C11–C12	109.0(6)	114.0
O4–C12–C11	107.2(6)	108.7
O4–C13–C14	126.1(7)	125.1
O4–C13–C18	115.1(6)	115.4
C14–C13–C18	118.8(7)	119.6
C13–C14–C15	119.9(7)	120.4
C14–C15–C16	121.7(7)	120.0
C15–C16–C17	118.9(8)	120.1
C16–C17–C18	120.0(7)	120.4
O5–C18–C13	115.1(6)	115.4
O5–C18–C17	124.3(6)	125.1
C13–C18–C17	120.5(6)	119.5
O5–C19–C1	107.4(5)	108.3
O6–C20–N1	112.5(6)	112.5
N3–C21–C22	109.5(7)	108.6
N3–C21–C26	129.6(8)	130.7
C22–C21–C26	121.0(8)	120.7
N1–C22–C21	103.5(7)	103.7
N1–C22–C23	134.3(7)	134.0
C21–C22–C23	122.2(7)	122.3
C22–C23–C24	114.5(8)	116.2
C23–C24–C25	122.8(9)	122.0
C24–C25–C26	123.4(9)	121.4
C21–C26–C25	116.1(8)	117.3

result in the termination of the calculations. It was also found that the calculations could achieve convergence more rapidly, if the input data were closer to the experimental values of the minimal energy points of the molecules. The converged calculations can then provide the optimal geometric bond length, bond angle, and dihedral angle of the eight LCEs.

### 3.3. Orbital field energy, vibrational frequency, and thermodynamic properties

Using the optimized geometry, thermodynamic properties of orbital energy, vibrational frequency, ionization energy, energy gap between HOMO–LUMO, atomic heat, enthalpy and Gibbs energy, etc., of each LCEs were calculated. The results were then used to determine the relative stability of the different sidearm of the eight LCEs. Therefore, the resulting molecular stability and conductivity are of special importance and value.

## 4. Results and discussions

### 4.1. Geometric structure

The structure of molecules plays an especially significant role in determining their chemical properties. As a result, the optimization of the compound is particularly important. The obtained geometric structure of eight c-pivot lariat crown ethers is shown in Fig. 1. Through structural analysis, using X-ray crystallography, the ORTEP dia-

grams of the four lariat crown ethers 1–4 were identified and shown in Figs. 2–5. The structures of the four lariat crown ethers show different crystal systems and space groups. The three-dimensional coordinates of the X-ray structural analysis were also used as input data for theoretical calculations. AM1 semi-empirical method was first used to conduct calculations until convergence was achieved. The geometric optimization was then conducted using the 6-31G\* BSF and the B3LYP method. Tables 1–4 provide the resulting bond lengths of the LCEs 1–4 from the X-ray crystallography structural analysis and theoretical calculations. Similarly, Tables 5–8 provide the torsion angles obtained using the X-ray crystallography structural analysis and theoretical calculations. In addition, Table 9 provides the crystallographic data collected during the study. These tables show that both the bond lengths and torsion angles obtained from the theoretical calculations are in good agreement with those from experimental investigations using X-ray crystallography. Tables 10–13 provide the resulting bond lengths and torsion angles of the LCEs 5–8 from the DFT theoretical calculations.

### 4.2. Molecular first ionization potentials, HOMO and LUMO energies, energy gaps

Table 14 lists the calculated values of the first ionization potentials, HOMO, LUMO, and energy gap ( $\Delta\epsilon_{\text{HOMO-LUMO}}$ ) of the eight LCEs. From the data, the first ionization potential of 8 was found to be the lowest. On the other hand, the energy gap of 4 was found to be the lowest, indi-

Table 9  
Crystallographic data

	1	2	3	4
Empirical formula	C <sub>25</sub> H <sub>27</sub> NO <sub>6</sub>	C <sub>30</sub> H <sub>30</sub> O <sub>6</sub>	C <sub>26</sub> H <sub>28</sub> O <sub>9</sub> S	C <sub>26</sub> H <sub>27</sub> N <sub>3</sub> O <sub>6</sub>
Formula weight	437.49	486.53	516.56	477.51
Crystal system	Orthorhombic	Orthorhombic	Monoclinic	Monoclinic
Space group	P2(1)2(1)2(1)	P2(1)2(1)2(1)	P2(1)/n	P2(1)/a
Unit cell dimensions (Å)	<i>a</i> = 7.888(2) <i>b</i> = 11.652(4) <i>c</i> = 24.416(4)	<i>a</i> = 7.3950(8) <i>b</i> = 15.745(3) <i>c</i> = 22.214(5)	<i>a</i> = 12.235(2) <i>b</i> = 7.674(3) <i>c</i> = 27.235(7)	<i>a</i> = 8.245(5) <i>b</i> = 27.549(5) <i>c</i> = 10.406(3)
$\beta$ (°)	90.00	90.00	94.37	96.23
Volume (Å <sup>3</sup> )	2244(1)	2587(1)	2550(1)	2350(2)
Z (atoms/unit cell)	4	4	4	4
<i>D</i> <sub>calc</sub> /mg m <sup>-3</sup>	1.295	1.249	1.346	1.350
<i>M</i> <sub>v</sub> /mm <sup>-1</sup>	0.09	0.09	0.18	0.10
<i>F</i> (0 0 0)	928	1032	1088	1008
Range of 2 $\theta$ /deg	49.8	51.8	51.8	53.8
Crystal size	0.35 × 0.20 × 0.15 mm	0.35 × 0.20 × 0.10 mm	0.45 × 0.25 × 0.15 mm	0.50 × 0.20 × 0.03 mm
Octants measured	<i>h</i> (0 to 9) <i>k</i> (0 to 130) <i>l</i> (0 to 29)	<i>h</i> (0 to 9) <i>k</i> (0 to 19) <i>l</i> (0 to 27)	<i>h</i> (–15 to 15) <i>k</i> (0 to 9) <i>l</i> (0 to 33)	<i>h</i> (–10 to 10) <i>k</i> (0 to 35) <i>l</i> (0 to 13)
Number of reflections measured	2277	2897	5096	5361
Number of unique reflection	2277	2897	4990	5091
Number of reflections with <i>I</i> > 2.5 or 2.0 $\sigma$ ( <i>I</i> )	1866	1432	2488	1665
Number of variables	290	326	326	226
Absorption correction	0.862–0.976	0.755–0.792	0.812–0.949	0.911–0.974
<i>R</i> <sub>f</sub>	0.037	0.037	0.049	0.067
<i>R</i> <sub>w</sub>	0.034	0.028	0.048	0.066
GoF	1.255	1.581	0.807	0.665

cating higher conductivity. Table 14 also shows that **3** has the highest first ionization potential whilst **5** has the highest energy gap.

#### 4.3. Thermodynamic properties

The DFT calculation shows that  $\Delta H_f$  are between  $-3004.726$  and  $-3666.124$  kcal mol<sup>-1</sup> for the eight LCEs. However, the calculated  $\Delta G_f$  are between  $-2778.627$  and  $-3329.091$  kcal mol<sup>-1</sup> for the eight LCEs. Additionally, the obtained thermodynamic parameter of eight c-pivot lariat crown ethers is shown in Fig. 6. In general, the formation of the eight LCEs is exothermic ( $\Delta H < 0$ ) and also causes

LCEs to be more rigid, and this is probably the reason that the entropy change for the reaction is slightly negative. However, the change in the enthalpy is big and negative enough to overcome the negative change of entropy. In addition, the results also show that the eight different LCEs are stable and easy-to-form molecules with high reactivity. Calculations also indicate that **8** is formed most readily and is also the most stable (Table 15).

#### 4.4. Vibrational frequencies

The calculated vibrational frequencies of the eight different geometric structures of the LCEs are all positive, indi-

Table 10

Optimized structure of lariat crown ether **5** located using B3LYP/6-31G\* calculations for atomic bond lengths (Å) and atomic torsion angle (°)

Atomic bond lengths (Å)		Atomic torsion angle (°)	
C1–C2	1.400	C2–C1–C6	119.8
C1–C6	1.398	C1–C2–C3	120.7
C2–C3	1.392	C2–C3–C4	119.4
C2–C3	1.392	C3–C4–C5	120.6
C3–C4	1.398	C4–C5–C6	119.9
C4–C5	1.391	C4–C5–O1	119.7
C5–C6	1.413	C6–C5–O1	120.3
C5–O1	1.378	C1–C6–C5	119.5
C6–O4	1.371	C1–C6–O4	125.3
O1–C7	1.436	C5–C6–O4	115.2
C7–C8	1.523	C5–O1–C7	115.9
C8–O2	1.415	O1–C7–C8	109.3
O2–C9	1.424	C7–C8–O2	114.2
C9–C10	1.520	C8–O2–C9	115.4
C10–O3	1.434	O2–C9–C10	106.2
O3–C13	1.373	C9–C10–O3	107.3
C11–C12	1.397	C10–O3–C13	115.6
C11–C16	1.400	C12–C11C16	120.1
C12–C13	1.413	C11–C12–C13	119.5
C12–O5	1.371	C11–C12–O5	124.7
C13–C14	1.391	O3–C13–C14	119.8
C14–C15	1.398	C12–C13–C14	119.6
C15–C16	1.391	C13–C14–C15	120.8
O4–C24	1.529	C14–C15–C16	119.5
C17–C18	1.393	C11–C16–C15	120.5
C17–C22	1.405	C6–O4–C24	119.5
C18–C19	1.406	C18–C17–C22	119.3
C18–O7	1.364	C17–C18–C19	120.6
C19–C20	1.387	C17–C18–O7	124.1
C20–C21	1.406	C18–C19–C20	119.6
C20–C26	1.514	C19–C20–C26	120.8
C21–C22	1.395	C21–C20–C26	118.5
C22–O8	1.366	C20–C21–C22	119.2
O5–C23	1.419	C17–C22–C21	120.7
C23–C25	1.535	C17–C22–O8	114.7
C24–C25	1.552	C21–C22–O8	124.5
C25–O6	1.426	C12–O5–C23	118.6
O6–C26	1.423	O5–C23–C25	106.6
O7–C27	1.419	O4–C24–C25	112.9
O8–C28	1.418	C23–C25–C24	113.1
		C23–C25–O6	111.5
		C24–C25–O6	113.0
		C25–O6–C26	117.2
		C20–C26–O6	109.8
		C18–O7–C27	118.3
		C22–O8–C28	118.3

Table 11

Optimized structure of lariat crown ether **6** located using B3LYP/6-31G\* calculations for atomic bond lengths (Å) and atomic torsion angle (°)

Atomic bond lengths (Å)		Atomic torsion angle (°)	
C1–C2	1.388	C2–C1–C6	121.1
C1–C6	1.401	C1–C2–C3	119.9
C2–C3	1.401	C2–C3–C4	120.5
C3–C4	1.393	C3–C4–C5	119.6
C4–C5	1.419	C3–C4–O1	124.7
C4–O1	1.367	C5–C4–O1	115.7
C5–C6	1.394	C4–C5–C6	119.3
C5–C17	1.369	C4–C5–O4	116.0
O1–C6	1.423	C6–C5–O4	124.8
C7–C8	1.524	C1–C6–C5	120.6
C8–O2	1.415	C4–O1–C7	119.0
O2–C9	1.423	O1–C7–C8	108.8
C9–C10	1.522	C7–C8–O2	114.0
C10–O3	1.425	C8–O2–C9	113.7
O3–C12	1.364	O2–C9–C10	108.0
C11–C12	1.412	C9–C10–O3	104.7
C11–C16	1.391	C10–O3–C12	119.7
C11–O4	1.379	C12–C11C16	119.8
C12–C13	1.396	C12–C11–O5	120.0
C13–C14	1.399	C16–C11–O5	120.1
C14–C15	1.393	O3–C12–C11	115.5
C15–C16	1.399	O3–C12–C13	124.9
O4–C17	1.424	C11–C12–C13	119.6
C17–C18	1.533	C12–C13–C14	119.9
C18–C19	1.526	C13–C14–C15	120.5
C18–O6	1.420	C14–C15–C16	119.6
C19–O5	1.436	C11–C16–C15	120.5
O6–C20	1.427	C5–O4–C17	117.9
C20–C21	1.524	O4–C17–C18	109.0
C21–C22	1.541	C17–C18–C19	110.8
C22–C27	1.514	C17–C18–O6	104.4
C23–C24	1.396	C19–C18–O6	112.9
C23–C28	1.395	C18–C19–O5	109.6
C24–C25	1.396	C11–O5–C19	115.0
C25–C26	1.396	C18–O6–C20	116.2
C26–C27	1.401	O6–C20–C21	107.8
C27–C28	1.402	C20–C21–C22	112.3
		C21–C22–C27	112.8
		C24–C23–C28	120.1
		C23–C24–C25	119.5
		C24–C25–C26	120.1
		C25–C26–C27	121.0
		C22–C27–C26	120.9
		C22–C27–C28	120.8
		C26–C27–C28	118.2
		C23–C28–C27	121.0

cating that these molecules are located at the minimal points of the potential energy surfaces, indicating that all eight different LCEs are very stable molecules. The calculated maximum frequencies are between 3227.364 and 3244.571  $\text{cm}^{-1}$  for the eight LCEs, and among the calculated values, compound **4** is found to have the lowest frequency (10.201  $\text{cm}^{-1}$ ).

## 5. Conclusions

Eight LCEs were synthesized and optimal geometric structures were determined by experimental study and

Table 12  
Optimized structure of lariat crown ether **7** located using B3LYP/6-31G\* calculations for atomic bond lengths (Å) and atomic torsion angle (°)

Atomic bond lengths (Å)		Atomic torsion angle (°)	
C1–C2	1.417	C2–C1–C6	119.4
C1–C6	1.393	C2–C1–O1	115.4
C1–O1	1.366	C6–C1–O1	125.2
C2–C3	1.392	C1–C2–C3	119.8
C2–O4	1.366	C1–C2–O4	115.3
C3–C4	1.401	C3–C2–O4	125.0
C4–C5	1.388	C2–C3–C4	120.3
C5–C6	1.402	C3–C4–C5	120.0
O1–C7	1.422	C4–C5–C6	120.1
C7–C8	1.523	C1–C6–C5	120.4
C8–O2	1.412	C1–O1–C7	118.7
O2–C9	1.425	O1–C7–C8	108.7
C9–C10	1.529	C7–C8–O2	114.8
C10–O3	1.432	C8–O2–C9	116.3
O3–C12	1.378	O2–C9–C10	106.6
C11–C12	1.411	C9–C10–O3	112.3
C11–C16	1.398	C10–O3–C13	115.8
C11–O4	1.367	C12–C11–C16	119.5
C12–C13	1.393	C12–C11–O5	116.0
C13–C14	1.398	C16–C11–O5	124.5
C14–C15	1.393	O3–C12–C11	118.7
C15–C16	1.398	O3–C12–C13	121.5
O4–C17	1.421	C11–C12–C13	119.8
C17–C18	1.529	C12–C13–C14	120.6
C18–C19	1.537	C13–C14–C15	119.6
C18–O6	1.419	C14–C15–C16	120.4
C19–O5	1.429	C11–C16–C15	120.2
O6–C20	1.424	C2–O4–C17	119.2
C20–C21	1.524	O4–C17–C18	106.3
C21–C22	1.523	C17–C18–C19	112.7
C22–O7	1.424	C17–C18–O6	105.8
O7–C23	1.367	C19–C18–O6	112.9
C23–C24	1.400	C18–C19–O5	107.1
C23–C28	1.403	C11–O5–C19	118.9
C24–C25	1.399	C18–O6–C20	114.3
C25–C26	1.393	O6–C20–C21	107.7
C26–C27	1.399	C20–C21–C22	112.2
C27–C28	1.390	C21–C22–O7	107.3
		C22–O7–C23	118.7
		O7–C23–C24	124.6
		O7–C23–C28	115.5
		C24–C23–C28	119.8
		C23–C24–C25	119.4
		C24–C25–C26	121.8
		C25–C26–C27	119.2
		C26–C27–C28	120.6
		C23–C28–C27	120.0

theoretical calculations. Furthermore, molecular structural conformation optimized at B3LYP/6-31G\* level of theory indicated that there was an existence of considerable difference in the energy of the eight LCEs. Moreover, we were computing an optimized structure for the eight different LCEs, which was also thermodynamically stable

Table 13  
Optimized structure of lariat crown ether **8** located using B3LYP/6-31G\* calculations for atomic bond lengths (Å) and atomic torsion angle (°)

Atomic bond lengths (Å)		Atomic torsion angle (°)	
O1–C1	1.421	C1–O1–C20	115.8
O1–C20	1.423	C2–O2–C3	117.9
O2–C6	1.423	C8–O3–C9	119.0
O2–C3	1.370	C10–O4–C11	113.7
O3–C8	1.367	C12–O5–C13	119.6
O3–C9	1.423	C18–O6–C19	115.0
O4–C10	1.415	O1–C1–C2	104.5
O4–C11	1.423	O1–C1–C19	112.8
O5–C12	1.426	C2–C1–C19	110.9
O5–C13	1.364	O2–C2–C1	108.9
O6–C18	1.380	O2–C3–C4	124.8
O6–C19	1.436	O2–C3–C8	115.9
C1–C2	1.533	C4–C3–C8	119.3
C1–C19	1.526	C3–C4–C5	120.6
C3–C4	1.394	C4–C5–C6	120.1
C3–C8	1.418	C5–C6–C7	119.9
C4–C5	1.401	C6–C7–C8	120.5
C5–C6	1.388	O3–C8–C3	115.7
C6–C7	1.401	O3–C8–C7	124.7
C7–C8	1.393	C3–C8–C5	119.6
C9–C10	1.524	O3–C9–C10	108.8
C11–C12	1.522	O4–C10–C9	114.0
C13–C14	1.396	O4–C11–C12	108.0
C13–C18	1.412	O5–C12–C11	119.5
C14–C15	1.399	O5–C13–C14	125.0
C15–C16	1.393	O5–C13–C19	115.4
C16–C17	1.399	C14–C13–C18	119.6
C20–C21	1.520	C13–C14–C15	119.9
C21–C22	1.420	C14–C15–C16	120.5
C21–C30	1.390	C16–C17–C18	120.4
C22–C23	1.373	O6–C18–C13	120.0
C23–C24	1.418	O6–C18–C17	120.1
C24–C25	1.421	C13–C18–C17	119.9
C24–C29	1.434	O6–C19–C1	109.5
C25–C26	1.376	O1–C20–C21	110.1
C26–C27	1.415	C20–C21–C22	119.2
C27–C28	1.378	C20–C21–C30	120.6
C28–C29	1.424	C22–C21–C30	120.2
C29–C30	1.435	C21–C22–C23	121.2
C30–C31	1.514	C22–C23–C24	120.7
		C23–C24–C25	121.7
		C23–C24–C29	118.8
		C25–C24–C29	119.5
		C24–C25–C26	121.1
		C25–C26–C27	119.7
		C26–C27–C28	120.5
		C27–C28–C29	121.4
		C24–C29–C28	117.8
		C24–C29–C30	119.8
		C28–C27–C30	122.5
		C21–C30–C29	119.4
		C21–C30–C31	121.6
		C29–C30–C31	118.9

Table 14

Comparison of HOMO, LUMO, energy gaps ( $\Delta\varepsilon_{\text{HOMO-LUMO}}$ ), and first ionization potentials of the eight LCEs (eV)

Molecule parameter	1	2	3	4	5	6	7	8
$\varepsilon_{\text{HOMO}}$	-5.6417	-5.6278	-5.7933	-5.6518	-5.7331	-5.6110	-5.6257	-5.4722
$\varepsilon_{\text{LUMO}}$	-0.3877	-0.8789	-0.5945	-1.0947	0.0473	0.1390	0.0207	-0.8247
$I_{\text{1st}}$	5.6417	5.6278	5.7933	5.6518	5.7331	5.6110	5.6257	5.4722
$\Delta\varepsilon_{\text{HOMO-LUMO}}$	5.2540	4.7490	5.1987	4.5771	5.7805	5.7500	5.6463	4.6475

Table 15

Comparison of calculated thermodynamic properties of the eight LCEs (298 K, kcal mol<sup>-1</sup>)

Molecule parameter	1	2	3	4	5	6	7	8
$\Delta H_{\text{f}}$	-3004.726	-3551.453	-3273.530	-3073.947	-3445.795	-3354.591	-3401.128	-3666.124
$\Delta G_{\text{f}}$	-2718.627	-3166.117	-2960.261	-2770.620	-3116.350	-3036.830	-3078.126	-3329.091
$\Delta H_{\text{a}}$	6241.252	7127.590	6673.034	6589.366	7092.909	6917.714	7006.246	7405.215
$\Delta G_{\text{a}}$	5737.038	6498.545	6123.080	6055.920	6512.582	6356.834	6436.245	6813.601

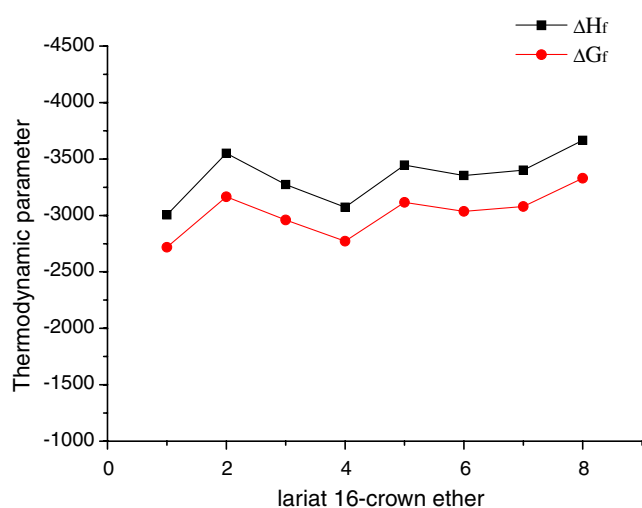


Fig. 6. Thermodynamic parameter of eight lariat 16-crown ethers.

and in excellent agreement with the experimental X-ray diffraction structure. Vibrational frequency analyses performed at the B3LYP/6-31G\* level of theory yielded zero imaginary frequency and confirms that all the optimized structures are in the ground state. The experimental results and density functional theory calculations (B3LYP) also established the electronic structures of these species and provided insight into the molecular mechanics. From theoretical calculations that use the B3LYP/6-31G\* density function method, data of the eight LCEs conformational analysis were successfully obtained. From these calculated and analytical results, the main results of the present study are summarized as follows.

- (1) The calculated bond lengths and torsion angles of the different eight LCEs are very close to the experimental values and are quite well and rational. These results prove that the calculations of optimal geometric three-dimensional structure of the eight compounds were successful.
- (2) Through the calculations of the first ionization potentials, HOMO, LUMO, and energy gaps, it was found

that the different eight LCEs have low energy gaps and low first ionization potentials. The electrons on the outermost molecular orbital are therefore more easily lost, indicating higher conductivity.

- (3) The calculations of thermodynamic properties and vibrational frequencies show that the different eight LCEs are all located at the stable, minimum points of the potential energy surfaces. They are all therefore stable structural LCEs with high reactivity.
- (4) The eight LCEs have the same parent macrocycle but contain different sidearms. When the sidearm of the lariat crown ether is changed, the thermodynamic properties of the ether would change significantly as well. Thus, the sidearm effect appears to be a strong influence on the metal ion binding capability.

The results of the DFT calculations are in good agreement with the experimental data, indicating that the method and basis set selected are feasible for calculating such large molecules. The DFT method appears to provide results that were in better agreement with the experimental results. In addition, the calculated geometries are considered to be accurate enough. The sidearm effect of the lariat 16-crown-5 ethers can also result in higher difference in the relative energy. Therefore, with different sidearms resulting in conformational change, different complex ability between lariat crown ethers and metals will be shown.

This research was performed to investigate the conformational preferences of the eight LCEs that can be applied as building blocks of the lariat crown ether macrocycles. The results of this study of high-density, high-energy lariat crown ethers should provide contribution to other members of this versatile new class of macrocycles.

#### Acknowledgements

The authors thank the National Science Council of the Republic of China (Taiwan) for its financial support (NSC 95-2113-M-012-001). The helpful suggestions from

Operator T.S. Kuo of National Taiwan Normal University, Department of Chemistry, are greatly appreciated. Dr. Y.C. Su, P.E., of Houston, Texas, USA, is also greatly appreciated for a critical reading of this manuscript prior to publication.

#### Appendix A. Supplementary data

Supplementary data associated with this article can be found, in the online version, at [doi:10.1016/j.molstruc.2006.07.035](https://doi.org/10.1016/j.molstruc.2006.07.035).

#### References

- [1] A. Lüttringhaus, *Ann. Chem.* 528 (1937) 181.
- [2] C.J. Pedersen, *J. Am. Chem. Soc.* 89 (1967) 7017.
- [3] W.S. Tang, X.X. Lu, K.M.C. Wong, V.W.W. Yam, *J. Mater. Chem.* 15 (2005) 2714.
- [4] W.J. Wang, E.V. Ganin, M.S. Fonari, Y.A. Simonov, G. Bocelli, *Org. Biomol. Chem.* 3 (2005) 3054.
- [5] S. Kongsuk, T. Kerdcharoen, S. Hannongbua, *J. Phys. Chem. B* 107 (2003) 4175.
- [6] D. Soto-Castro, P. Guadarrama, *J. Comput. Chem.* 25 (2005) 1215.
- [7] K. Janus, J. Sworakowski, *J. Phys. Chem. B* 109 (2005) 93.
- [8] A.A. El-Azhary, A.A. Al-Kahtani, *J. Phys. Chem. A* 109 (2005) 4505.
- [9] A. Casnati, N.D. Ca', F. Sansone, F. Ugozzoli, R. Ungaro, *Tetrahedron* 60 (2004) 7869.
- [10] S.T. Liddle, W. Clegg, C.A. Morrison, *Dalton Trans.* (2004) 2514.
- [11] E.S. Stoyanov, C.A. Reed, *J. Phys. Chem. A* 108 (2004) 907.
- [12] R. Chitta, L.M. Rogers, A. Wanklyn, P.A. Karr, P.K. Kahol, M.E. Zandler, F. D'Souza, *Inorg. Chem.* 43 (2004) 6969.
- [13] M. González-Lorenzo, C. Platas-Iglesias, F. Avecilla, S. Faulkner, S.J.A. Pope, A. de Bias, T. Rodríguez-Bias, *Inorg. Chem.* 44 (2005) 4254.
- [14] A. Frontera, M. Orell, C. Garau, D. Quiniñero, E. Molins, I. Mata, J. Morey, *Org. Lett.* 7 (2005) 1437.
- [15] M. Montejo, S.L. Hinchley, A.B. Altabef, H.E. Robertson, F.P. Ureña, D.W.H. Rankin, J.L. González, *Phys. Chem. Chem. Phys.* 8 (2006) 477.
- [16] C. Emmeluth, V. Dyczmons, T. Kinzel, P. Botschwina, M.A. Suhm, M. Yáñez, *Phys. Chem. Chem. Phys.* 7 (2005) 991.
- [17] T.S. Hofer, B.R. Randolf, B.M. Rode, *Phys. Chem. Chem. Phys.* 7 (2005) 1382.
- [18] U. Koert, *Phys. Chem. Chem. Phys.* 7 (2005) 1501.
- [19] A. Lenz, L. Ojamäe, *Phys. Chem. Chem. Phys.* 7 (2005) 1905.
- [20] H. Zhou, Z.H. Peng, Z.Q. Pan, D.C. Li, B. Liu, Z. Zhang, R.A. Chi, *J. Mol. Struct.* 743 (2005) 59.
- [21] K.K. Laali, V.D. Sarca, T. Okazaki, A. Brock, P. Der, *Org. Biomol. Chem.* 3 (2005) 1034.
- [22] S.L. Richardson, T. Baruah, M.J. Mehl, M.R. Pederson, *Chem. Phys. Lett.* 403 (2005) 83.
- [23] T. Sordo, P. Campomanes, A. Diéguez, F. Rodríguez, F.J. Fañanás, *J. Am. Chem. Soc.* 127 (2005) 944.
- [24] Q.S. Li, X.J. Feng, Y. Xie, H.F. Schaefer III, *J. Phys. Chem. A* 109 (2005) 1454.
- [25] H. Shirota, *J. Phys. Chem. B* 109 (2005) 7053.
- [26] S.M. Godfrey, A. Hinchliffe, A. Mkadmh, *Dalton Trans.* (2005) 1675.
- [27] C.C. Su, L.H. Lu, L. Kao-Liu, *J. Phys. Chem. A* 107 (2003) 4563.
- [28] C.C. Su, L.H. Lu, *J. Mol. Struct.* 702 (2004) 23.
- [29] T.J. Hsieh, L.H. Lu, C.C. Su, *Biophys. Chem.* 114 (2005) 23.
- [30] T.J. Hsieh, C.C. Su, C.Y. Chen, C.H. Liou, L.H. Lu, *J. Mol. Struct.* 741 (2005) 193.
- [31] (a) E.P. Kyba, R.C. Helegeson, K. Madan, G.W. Gokel, T.L. Tarnowski, S.S. Moore, D.J. Cram, *J. Am. Chem. Soc.* 99 (1979) 2564;  
(b) G.S. Heo, R.A. Bartsch, L.L. Schobohm, J.G. Lee, *J. Org. Chem.* 46 (1981) 3574.